NORMALIZATION OF TRANSCRANIAL MAGNETIC STIMULATION POINTS BY MEANS OF ATLAS REGISTRATION

D. Zosso[1]*, Q. Noirhomme*[2]*, M. Davare*[3]*, B. Macq*[2]*, E. Olivier*[3]*, J. Thiran*[1] *and M. De Craene*[2]

[1] Signal Processing Institute, Ecole Polytechnique Fédérale de Lausanne (EPFL)
email: {dominique.zosso, jp.thiran}@epfl.ch

[2] Communications and Remote Sensing Laboratory, Université catholique de Louvain
email: {noirhomme, macq, decraene}@tele.ucl.ac.be

[3] Neurophysiology Unit, Université catholique de Louvain
email: {davare, olivier}@nefy.ucl.ac.be

ABSTRACT

Transcranial magnetic stimulation (TMS) is a well-known technique to study brain function. Location of TMS points can be visualized on the subject's Magnetic Resonance Image (MRI). However inter-subject comparison is possible only after a normalization i.e. a transformation of the stimulation points to a reference atlas image.

Here, we propose a generic and automatic image processing pipe-line for normalizing a collection of subjects' MRI and TMS points. The normalization uses a loop of rigid-transform followed by Basis-Splines registration. The used reference atlas is the common Montreal National Institute (MNI) brain atlas [2]. We show preliminary results from 10 subjects. Those normalized points were compared to the SPM normalization and validated by TMS experts.

1. INTRODUCTION

In neuroscience, the function of a given cortical area can be studied by exploring the consequences of transcranial magnetic stimulation (TMS) on tasks under investigation, e.g. grasping an object or mental computation. In the TMS technique [4], the stimulation is induced by a coil, placed tangentially over the surface of the skull. When triggered, an important transient current passes through the coil and induces a magnetic field, activating underlying cortical brain areas and interfering with their normal function.

In order to obtain reproducibility and to enable inter-subject comparison, TMS points must be expressed within a common brain reference. Different brain references exist and are used within the neuroimaging community. One of the first references used is the Talairach stereotaxic system based on post mortem histological sections of the brain of a 60-year-old female subject [11]. The Montreal Neurological Institute (MNI) created a composite MRI dataset from 305 young normal subjects whose scans were individually mapped into the Talairach system (MNI305) [2]. Furthermore, one of the MNI lab members, Colin Holmes, was scanned 27 times (Colin27). Those scans were registered and averaged to create a very high detailed MRI dataset of one brain and were then matched to the MNI305. The current version of the well-known SPM, a statistical parametric mapping software commonly used in the functional brain imaging community, uses the reference "ICBM152", the average of 152 normal MRI scans that have also been matched to the MNI305.

The process of mapping TMS coordinates from the subject image into the atlas reference system is called *normalization*. The inverse process is designated as *denormalization*. Solving the normalization and denormalization problems is thus equivalent to finding the best spatial transformation for establishing a correspondence between the subject and the atlas space of coordinates. In this study, we propose the use of a generic and automatic image registration technique for addressing these problems.

Image registration is the concept of mapping homologous points of different images representing a same object. In image processing the abstract definition of homology is substituted by a measurable criterion of image similarity, evaluated by means of an image-to-image metric.

Talairach [11] defined a brain coordinate system whose origin is placed at the anterior commissure (AC) and such that the line joining anterior and posterior commissure (PC) is horizontal. After this global alignment, the Talairach transform maps brains of different shape and size using quadrant by quadrant linear scaling.

Friston et al. [3] proposed kernel convolutive intensity normalization and non-rigid spatial transformations using basis functions. They linearize the image matching equation in order to obtain an algebraic solution in terms of least squares. This approach is the method used in SPM.

A more generic approach defines image registration as an iterative optimization, modifying the parameters of a transform in order to improve a given image-to-image metric between a fixed and a transformed moving image [7]. This method is useful where the linearization hypotheses underlying Friston's algebraic formulation do not hold and is implemented in the widely used Insight Segmentation and Registration Toolkit (ITK) [5].

We have chosen this general approach in order to use a metric different than least-squares and more suitable to multimodality. Further we iteratively establish registration rather than to use a first guess. Our registration method can equally be applied to most other types of medical image, including CT scan, PET or fMRI.

The paper is organized as follows. We first present our normalization approach, based on the chaining of affine and B-Splines transformation models. We then present sample results of 10 subject image to atlas registration, as well as their corresponding TMS point normalizations. Finally, we discuss and compare our results with those provided by the semi-automatic SPM approach [3].

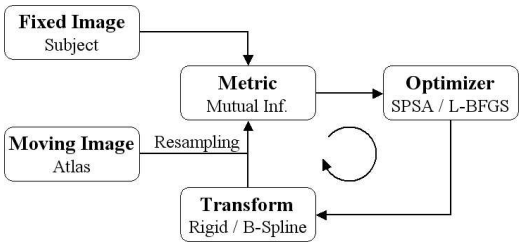

Figure 1: Image registration as an optimization loop. The optimization loop consists of an optimizer that modifi es the parameters of a transform in order to improve the image-to-image metric. Two different transform models are used, each of which has a different optimizer that corresponds.

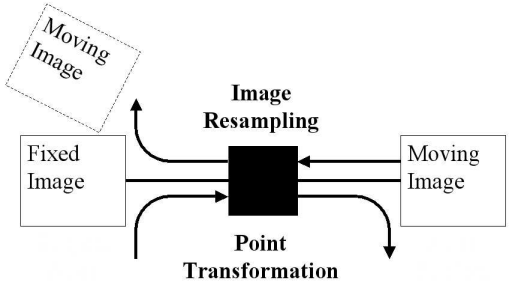

Figure 2: Image configuration for non-invertible registration. Fixed and moving image have to be set in order to correspond to the desired transform direction. Image resampling takes place in the opposite direction (dashed line).

2. METHODS

2.1 TMS Acquisition

The normalization is tested on TMS points acquired in 10 subjects. Four brain areas, namely the left (L) or right (R) ventral (PMv) and dorsal (PMd) premotor cortex, are selected to test their respective contribution to precision grasping [1]. Stimulation point coordinates are acquired using a magnetic field digitizer. They are registered with the corresponding subject MRI, as described in [9]. After the normalization procedure, we expect to find all points from given brain area to be located on the same position on the Colin27 atlas.

2.2 Brain Images

Images, which the native TMS coordinates refer to, are acquired for each subject. They are T1-weighted MR head scans of different resolutions and non-uniform field of view. At acquisition, subject images are oriented for the anterior and posterior commissure to be located on the same axial slice. Image origin (physical space) is placed at the pixel in the lower left posterior image corner (0, 0, 0).

The reference used in the current application is Colin27. The image is a MRI T1 acquisition with uniform spacing of 1 mm per pixel. Its physical origin is located in the AC, at voxel (90, 126, 72).

2.3 Image Registration Pipeline

The structure of the image registration process we use is illustrated in figure 1. For normalization, the subject image is fixed, and one wants to find the transform that best maps its points into the moving atlas image. We define the following optimization loop: The moving image is resampled using the current spatial transform estimation, and compared to the fixed image by means of the mutual information image-to-image metric. An optimizer block evaluates the metric, estimates its gradient and possibly its Hessian, and tunes the parameters of the transform. Iteratively, the spatial transform leading to an image similarity optimum is established.

2.3.1 Image Resampling and Transform Direction

The transform being optimized maps points of the fixed image physical space into the moving image physical space. When resampling the moving image, for the whole reference image the intensities of corresponding points in the moving image are looked up.

The deformable transform model is non invertible and transformations are only possible in one direction. The image configuration is imposed by the further use of the output transform, as illustrated in figure 2:

- For normalization, TMS coordinates are transformed from subject to atlas. The subject image is setup as fixed image and the atlas is the moving image.
- For denormalization, TMS coordinates are mapped from the atlas reference into the subject coordinate system. Therefore, the atlas constitutes the fixed image while the subject image is moving.

2.3.2 Transform Models

First, we use a rigid transformation that accounts for global misalignment (rotation and translation). After this initialization, a deformable transform model is used to establish local homology, correcting local deformations and differences in size and proportion.

Rigid Transform Model. The space of possible transformations is reduced to rigid and affine transforms. We define a rigid transformation as rotation about the center c, followed by translation t. The m-dimensional transform of a point P can be written as follows:

$$T(P) = \mathbf{A}(P-c)+c+t \tag{1}$$

where $\mathbf{A} = \mathbf{SR}$ is the product of the diagonal scaling matrix $\mathbf{S}$ and the rotation matrix $\mathbf{R}$. Such a transform counts $4m$ parameters and is therefore particularly simple. Further it is analytically defined for any point.

A gradient descent method is appropriate to run the optimization. We use the simultaneous perturbation stochastic approximation (SPSA) method, which allows for a faster gradient estimation than classical steepest descent implementations [10].

B-Spline Deformable Transform. B-Spline deformable transform is a semi-free-form transform. Deformation vectors are placed on a uniform grid. These vectors are the parameters modified during the optimization process. The dense deformation field is interpolated using B-Splines.

Using a smooth third-order basis spline, interpolation can be calculated on 3 nodes less than are present in the grid along each dimension. For a 3D image and $n = 10$ effective grid points per dimension, the number of transform parameters is $p = 6591$. We use an implementation of the quasi-Newton limited memory Broyden-Fletcher-Goldfarb-Shanno optimization algorithm (L-BFGS) [6] to handle this huge parameter space.

2.3.3 *Mutual Information Image-to-Image Metric*

The use of mutual information (MI) as an image metric has been introduced by Viola and Wells. The two images are considered as two discrete random variables, X and Y. Mutual information is defined as follows:

$$MI(X,Y) = H(X) + H(Y) - H(X,Y) \tag{2}$$

where $H(X,Y)$ is the joint entropy of the two images and $H(X)$, $H(Y)$ their respective marginal entropy. MI can be interpreted as the loss of uncertainty obtained when considering both images jointly, compared to observing them independently.

Maximum MI can be obtained for matched images whose intensities are not equal, but mapped in a bijective way, i.e. there exists a bijective function that maps the intensities of I_1 to the intensities of I_2. This characteristic is interesting when comparing images of different modalities.

While Viola-Wells propose Parzen-window PDF estimation, Mattes establishes the joint histogram of the fixed and the moving image using B-Spline kernels [8]. Along the fixed image dimension, smoothing is not necessary as no interpolation and derivation takes place. Along the moving image dimension, however, a third order B-Spline kernel is used, giving rise to a smooth histogram with continuous gradient, which is important in derivative calculation:

$$q(i_1,i_2) = \frac{1}{N}\sum_{\mathbf{x}} \beta^1\left(i_1 - \frac{I_1(\mathbf{x}) - \min(I_1)}{\Delta i_1}\right) \cdot \beta^3\left(i_2 - \frac{I_2(\mathbf{x}) - \min(I_2)}{\Delta i_2}\right) \tag{3}$$

where β^n is the n^{th}-order B-Spline, $\min(I_{\{1,2\}})$ the least pixel intensity of the images and $\Delta i_{\{1,2\}} = (\max I_{\{1,2\}} - \min I_{\{1,2\}})/h_{\{1,2\}}$ the respective histogram bin size, $h_{\{1,2\}}$ being the corresponding number of histogram bins. Marginal PDF are calculated by summing the joint PDF along the complementary dimensions.

The Mattes normalization with respect to the minimal and maximal intensity value in an image makes this approach particularly interesting, as fewer image pre-processing is necessary, which makes it the implementation of our choice.

2.3.4 *Model Cascading*

When cascading, transforms are ideally passed to the subsequent image registration step under their analytical form. However, to simplify the implementation and for easier modularity, the output transform of the first step is applied to resample the moving image as an approximation of the fixed image and this resampled output image serves as moving image of the subsequent registration step. This is illustrated in figure 3 a).

2.4 TMS Point Transformation

Once the spatial correspondence between the subject and atlas image is established, the transform can be used to map points from the fixed image reference into the moving image space.

Compared to image registration, transforms have to be applied in reverse order to each of the acquired TMS points. First, the B-Spline deformable model transforms TMS points from fixed image into the intermediate rigid and scale estimation, and second, the rigid and scale transform maps into the native atlas reference space, as illustrated in figure 3 b).

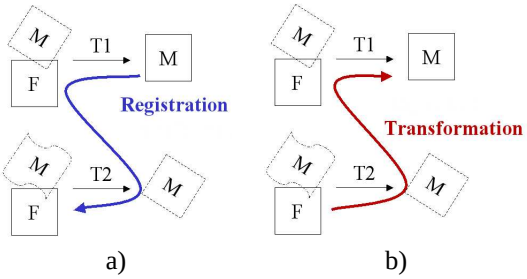

Figure 3: Cascading image registration steps. *a)* Rigid and scale transformation T_1 is established. The resampled image is used as moving image of the second registration step T_2 and resampled a second time (dash-dotted line). *b)* To map a point from fixed image space to original moving image space, transforms are applied in reverse order.

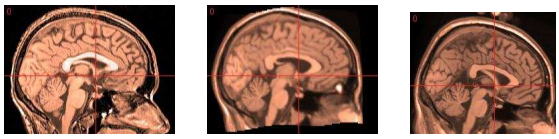

Figure 4: Brain MRI images resulting from subject-atlas registration. *a)* Original native subject MRI. *b)* Normalization transformation applied to Colin27. *c)* Original atlas (Colin27).

3. RESULTS

3.1 MRI Subject-Atlas Registration

In figure 4 resulting warped images for one subject-atlas registration are illustrated.

3.2 TMS Point Normalization

Stimulation points from ten different subjects have been normalized after image registration. Their sample means corresponding to each of the four brain areas are calculated. The complete normalized set has been projected on a 3D rendering of the atlas brain (figure 5).

More detailed analysis of obtained data and its dispersion is done by calculation of the covariance matrix Σ for the four populations. Main directions of dispersion can be obtained when proceeding to an eigenvector decomposition. This decomposition yields the two matrices V and D that verify $\Sigma = VDV^{-1}$, where V is the orthonormal matrix whose columns contain the eigenvectors of Σ, and D is the diagonal matrix composed of the corresponding eigenvalues. Standard deviation along the established main dispersion directions is given by the square root of the respective eigenvalue. Data are shown in table 1.

3.3 Comparison to Semi-Automatic Normalization Using SPM Registration

Every TMS point has equally been normalized using a semi-automatic approach based on SPM image registration. Subject and atlas images are registered using the spatial normalization method of the SPM package. In the resampled registered image, an expert manually identified the TMS points as they appeared in the native subject image. Both normalized sets are illustrated in figure 6. To compare both methods, the same covariance analysis and eigenvector decomposition has been done for the SPM normalization, as for our method before. Further, pairwise differences are calculated, giving

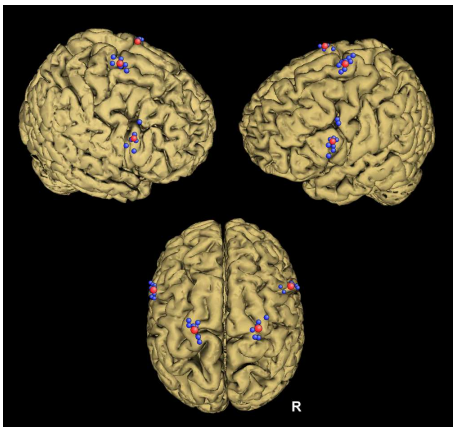

Figure 5: Normalized TMS points and sample mean. TMS points gathered from 10 subjects are normalized onto the atlas brain (small blue spheres, 10 on the left and 6 on the right hemisphere). The sample mean has been drawn as big red spheres.

	PMvR	PMvL
μ_{auto}	(61 , 11.6 , 21.3)	(-60.7 , 13.7 , 24.7)
Σ	$\begin{pmatrix} 10.3 & -6.5 & 2.3 \\ -6.5 & 11.3 & 1.6 \\ 2.3 & 1.6 & 43.9 \end{pmatrix}$	$\begin{pmatrix} 5.6 & 4.8 & 2.7 \\ 4.8 & 43.6 & -26.5 \\ 2.7 & -26.5 & 34.7 \end{pmatrix}$
V	$\begin{pmatrix} 0.732 & 0.679 & 0.062 \\ 0.678 & -0.735 & 0.038 \\ -0.071 & -0.014 & 0.997 \end{pmatrix}$	$\begin{pmatrix} 0.880 & 0.475 & -0.032 \\ -0.327 & 0.555 & -0.765 \\ -0.345 & 0.683 & 0.643 \end{pmatrix}$
D	$\begin{pmatrix} 4.091 & 0 & 0 \\ 0 & 17.322 & 0 \\ 0 & 0 & 44.111 \end{pmatrix}$	$\begin{pmatrix} 2.751 & 0 & 0 \\ 0 & 14.963 & 0 \\ 0 & 0 & 66.098 \end{pmatrix}$
σ	(2.02 , 4.16 , 6.64)	(1.66 , 3.87 , 8.13)

	PMdR	PMdL
μ_{auto}	(25.6 , -12.6 , 72.3)	(-26.8 , -9.8 , 70.7)
Σ	$\begin{pmatrix} 10.3 & -4.6 & -5.4 \\ -4.6 & 36.3 & -6.8 \\ -5.4 & -6.8 & 16.9 \end{pmatrix}$	$\begin{pmatrix} 22.8 & 6.0 & -0.4 \\ 6.0 & 49.7 & -14.7 \\ -0.4 & -14.7 & 12.5 \end{pmatrix}$
V	$\begin{pmatrix} 0.817 & 0.568 & -0.104 \\ 0.239 & -0.168 & 0.956 \\ 0.526 & -0.806 & -0.273 \end{pmatrix}$	$\begin{pmatrix} -0.106 & -0.979 & -0.172 \\ 0.338 & 0.127 & -0.933 \\ 0.935 & -0.157 & 0.318 \end{pmatrix}$
D	$\begin{pmatrix} 5.488 & 0 & 0 \\ 0 & 19.258 & 0 \\ 0 & 0 & 38.731 \end{pmatrix}$	$\begin{pmatrix} 7.179 & 0 & 0 \\ 0 & 22.011 & 0 \\ 0 & 0 & 55.843 \end{pmatrix}$
σ	(2.34 , 4.39 , 6.22)	(2.68 , 4.69 , 7.47)

Table 1: Dispersion analysis of normalized TMS points. The population mean is given by μ_{auto}. Σ denotes the respective estimated covariance matrix. V is the matrix containing the eigenvectors of Σ, indicating the main spatial directions of dispersion, respective variances are given by the diagonal eigenvalue matrix D. σ is the standard deviation in *mm* along the eigenvectors.

rise to indicators such as mean difference vectors and mean difference norms. Results are presented in table 2.

4. DISCUSSION

4.1 Image Registration

Mutual information is an appropriate image-to-image metric for brain MRI subject-atlas registration. Even if images have been acquired using theoretically equal MR weightings, they differ in intensities, which makes the use of rigid metrics, such as mean squared differences, inappropriate. Further, MI enables the later change of the atlas weighting or modality without important adaptation of the registration tool. The metric value can be used as a quality criterion of the registration, but interpretation of the metric value is not straightforward.

The results we obtained have been validated by experts in the domain of TMS research. Physicians carefully evaluated the registration results. They visually compared the resampled image to the target image. The position was checked for both left and right, ventral and dorsal premotor cortex. In general, most of the resampled atlas images correspond well to the original subject images, and image registration can be considered of good quality. However, several subjects reveal

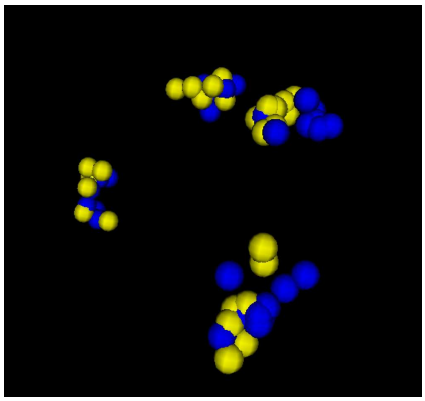

Figure 6: TMS point normalization comparison to SPM results. Automatic normalization results are drawn in blue. Yellow spheres represent results of SPM image registration and manual point identifi cation.

	PMvR	PMvL	PMdR	PMdL
μ_{SPM}	$\begin{pmatrix} 55.67 \\ 16.00 \\ 25.67 \end{pmatrix}$	$\begin{pmatrix} -59.60 \\ 16.30 \\ 23.20 \end{pmatrix}$	$\begin{pmatrix} 24.33 \\ -4.67 \\ 72.00 \end{pmatrix}$	$\begin{pmatrix} -22.30 \\ -4.20 \\ 71.40 \end{pmatrix}$
σ	$\begin{pmatrix} 2.32 \\ 5.75 \\ 8.85 \end{pmatrix}$	$\begin{pmatrix} 1.18 \\ 2.09 \\ 9.04 \end{pmatrix}$	$\begin{pmatrix} 2.38 \\ 2.78 \\ 6.51 \end{pmatrix}$	$\begin{pmatrix} 1.74 \\ 1.98 \\ 5.69 \end{pmatrix}$
$\mu_{\text{auto}} - \mu_{\text{SPM}}$	$\begin{pmatrix} 4.65 \\ -3.86 \\ -3.71 \end{pmatrix}$	$\begin{pmatrix} -1.16 \\ -2.59 \\ 1.46 \end{pmatrix}$	$\begin{pmatrix} 0.73 \\ -5.77 \\ -0.24 \end{pmatrix}$	$\begin{pmatrix} -4.54 \\ -5.45 \\ -0.62 \end{pmatrix}$
$\lVert\mu_{\text{auto}} - \mu_{\text{SPM}}\rVert$	7.09	3.19	5.82	7.12
$E(\lVert auto - SPM\rVert)$	9.19	7.81	8.08	11.05

Table 2: Comparison of TMS points normalization using SPM registration. The population mean is given by μ_{SPM}. σ is the standard deviation in *mm* along the main directions of dispersion. $\mu_{\text{auto}} - \mu_{\text{SPM}}$ denotes the difference vector between population means and $\lVert\mu_{\text{auto}} - \mu_{\text{SPM}}\rVert$ its norm. $E(\lVert auto - SPM\rVert)$ represents the mean distance between corresponding points.

some difficulties of the registration tool. In fact, some original images do not have exactly the same field of view and major parts of problematic regions are not represented in the atlas. To prevent the image registration process from being disturbed by such differences, prior masking of those critical regions would be necessary.

One of the main factors leading to successful image registration is that images do contain the same body parts (similar FOV) and that sufficient image margins are present.

If the transform is to be used in both directions, a pseudo-inverse has to be constructed, or registration has to be run with both configurations simultaneously. However, image registration with swapped image configuration is unlikely to yield symmetrical transformations. Subsequent normalization and denormalization of a TMS point will most probably differ from the original TMS point.

4.2 Normalization Dispersion

Low standard deviation of the normalized points indicate good registration quality. However, the contrary statement would not hold, as dispersion can be due to different causes, e.g.:

- Poor registration quality at normalization,
- Registration errors at point to image registration,
- Non precise point localization at acquisition,
- Structural differences between subjects (homologous points are not situated at topologically corresponding coordinates).

Dispersion analysis reveals interesting information about the main directions of spatial dispersion. In fact, spatial dis-

persion is not uniform. Standard deviation along the principal axes lies around 2, 4 and 8 mm respectively. The eigenvector corresponding to the direction of least standard deviation is oriented along the cortex surface normal. Both higher dispersion directions are in the plane tangential to the brain surface.

Along the normal direction, one intuitively expects least dispersion, as at each phase committed error is minimal: Registration is easier normal to contours rather than tangential, as stated by the aperture problem. Points are explicitly selected at the cortex surface, which leads to a weaker error injection at acquisition time.

Based on the current data it is impossible to conclude about the exact contributions of the different sources to the observed inplane dispersion. With an inplane standard deviation of around 4 and 8 mm respectively, the overall normalization quality can still be qualified as good.

4.3 Comparison to Semi-Automatic SPM Normalization

Dispersion analysis of the normalized TMS points based on SPM image registration followed by manual point identification yields standard deviation measures similar to the ones obtained with our presented method. This is an indicator of similar image registration quality.

Sample means of the four normalized point populations differ by 5 to 7 mm between our method and the SPM comparison. A horizontal shift in the anterior-posterior direction of 2.6 up to 5.8 mm is common to all four point sets, accounting for the major part of mean differences. Mean norms of pairwise difference vectors lie between 7.8 and 11 mm, which is almost double the distance between respective population means. This indicates a large random contribution to normalization differences.

5. CONCLUSIONS

In this paper we presented a fully automatic approach to spatial TMS point normalization using subject-atlas registration of brain MRI scans. A general subject-atlas registration framework has been developed that yields good quality spatial mapping of brain MRI. The presented registration pipeline consisting of, firstly, affine and, secondly, B-Spline deformable transforms allows for a good overall alignment of the represented structures. The established spatial transform is used to normalize coordinates of TMS points from native subject space into the reference atlas.

Normalized TMS coordinates are distributed over a well restricted brain region. The mean value and standard deviation are comparable to the results of semi-automatic expert-based normalizations. The accuracy of the image registration – and thereby of the TMS points normalization – can be further improved by masking regions that do not appear on both subject MRI and atlas.

The presented non-rigid deformation model is not able to handle very local structural differences, particularly where the hypothesis of homologous topology is not strictly valid. In order to obtain a more precise match of the cortical structures – gyri and sulci – more flexible deformation models would possibly improve normalization accuracy, for example by adding a third registration step consisting of a free-form voxel-based deformation model.

Since TMS coordinate normalization and denormalization only concern points situated on the cortical surface, one might imagine a registration procedure limited to cortical surfaces.

6. ACKNOWLEDGMENTS

The work of Q. Noirhomme and M. De Craene has been supported by the following grants from the Région Wallonne: POPSE (EPI A320501R0322/215092) and ASUR (EPI A320501R049F /415732).

REFERENCES

[1] M. Davare, M. Andres, J.-L. Thonnard, G. Cosnard, and E. Olivier. Dissociating the Role of Ventral and Dorsal Premotor Cortex in Precision Grasping. *Journal of Neuroscience*, 2006. In press.

[2] A.C. Evans, D.L. Collins, S.R. Mills, E.D. Brown, R.L. Kelly, and T.M. Peters. 3D Statistical Neuroanatomical Models from 305 MRI Volumes. In *Proceedings IEEE-Nuclear Science Symposium and Medical Imaging Conference*, pages 1813–1817, 1993.

[3] K.J. Friston, J. Ashburner, C.D. Frith, J.-B. Poline, J.D. Heather, and R.S.J. Frackowiak. Spatial Registration and Normalization of Images. *Human Brain Mapping*, 2:165–189, 1995.

[4] M. Hallet. Transcranial Magnetic Stimulation and the Human Brain. *Nature*, 406:147–150, July 2000.

[5] L. Ibanez, W. Schroeder, L. Ng, and J. Cates. *The ITK Software Guide*. Kitware, Inc. ISBN 1-930934-15-7, http://www.itk.org/ItkSoftwareGuide.pdf, second edition, 2005.

[6] D.C. Liu and J. Nocedal. On The Limited Memory BFGS Method for Large Scale Optimization. *Mathematical Programming*, 45:503–528, 1989.

[7] J. B. A. Maintz and M. A. Viergever. A survey of medical image registration. *Medical Image Analysis*, 2(1):1–36, 1998.

[8] D. Mattes, D.R. Haynor, H. Vesselle, T.K. Lewellen, and W. Eubank. Non-rigid Multimodality Image Registration. In *Proceedings SPIE, Medical Imaging 2001: Image Processing*, volume 4322, pages 1609–1620, Bellingham, WA, 2001.

[9] Q. Noirhomme, M. Ferrant, Y. Vandermeeren, E. Olivier, B. Macq, and O. Cuisenaire. Registration and Real-Time Visualization of Transcranial Magnetic Stimulation With 3-D MR Images. *IEEE Transactions on Biomedical Engineering*, 51:1994–2005, 2004.

[10] J.C. Spall. Multivariate Stochastic Approximation Using a Simultaneous Perturbation Gradient Approximation. *IEEE Transactions on Automated Control*, 37:332–341, 1992.

[11] J. Talairach and P. Tournoux. *Co-planar Stereotaxic Atlas of the Human Brain: 3-Dimensional Proportional System - an Approach to Cerebral Imaging*. Thieme Medical Publishers, New York, NY, 1988.